Properties and Evaluation of Functionalized Mixed Membrane Adsorbents for the Adsorption of Vanillic Acid from Palm Oil Waste

Zaharah Abdul Rahman[1], Nora'aini Ali[1,*], Sofiah Hamzah[1], Syed Mohd Saufi Tuan Chik[2], Norhafiza Ilyana Yatim[3], Siti Solihah Rasdei[1], Jan Setiawan[4]

[1] Faculty of Ocean Engineering Technology and Informatics, Universiti Malaysia Terengganu, 21300 Kuala Terengganu, Terengganu, Malaysia
[2] Faculty of Chemical & Natural Resources Engineering, Universiti Malaysia Pahang, Lebuhraya Tun Razak, 26300 Gambang, Pahang, Malaysia
[3] Higher Institution Centre of Excellence (HICoE), Institute of Tropical Aquaculture and Fisheries, Universiti Malaysia Terengganu, 21030 Kuala Nerus, Terengganu, Malaysia
[4] Electrical Engineering Department, Faculty of Engineering, Pamulang University, South Tangerang, Banten, Indonesia

ARTICLE INFO

ABSTRACT

Identifying factors that can improve the ability of mixed matrix membrane (MMM) adsorbents to isolate phenolic chemicals from palm oil waste is a major challenge. This study prepared a mixed matrix membrane with improved efficiency using a quaternary doping solution and a hydroxyapatite (HAp) filler and denoted as modified mixed matrix membrane (MMM_{HAp}). Prior to use, HAp powder obtained from eggshells calcined at different temperatures was evaluated as an absorbent for the desired phenolic compounds. All the prepared HAp and MMM_{HAp} powders were evaluated for their properties by Fourier transform infrared spectroscopy (FTIR), scanning electron microscope (SEM) and X-ray diffraction (XRD). For this study, vanillic acid was selected as a phenolic chemical because it is widely used in the pharmaceutical, biomedical and food industries. The optimal adsorption and vanillic acid isolation from crude palm oil samples by MMM_{HAp} occurred using an acetate buffer solution with a pH of 8. The data from the equilibrium adsorption study were also in agreement with the Freundlich isotherm, as the R^2 value was 0.9900 suggesting heterogeneous adsorption of vanillic acid on the surface of MMM_{HAp}. The kinetic adsorption study clearly shows a pseudo-second-order fit ($R^2=0.9992$), suggesting that chemisorption occurs between the adsorbed substance and the adsorbent. The modified membrane (MMM_{HAp}) has characteristics of its finger-like structures is more elongated and connected to the porous layer, indicating that the incorporation of hydroxyapatite nanoparticles into the membrane enhances the adsorption of vanillic acid from real sample and has the highest adsorption capacity of 170.8 mg/g. These results show that this improved MMM_{HAp} can be developed and used for waste utilization to obtain useful materials.

1. Introduction

Between 2019 and 2020, approximately 74.6 million tons of palm oil will be consumed worldwide, with Malaysia being one of the leading producers [1]. It is expected that the palm oil industry in

---

Malaysia will produce about 80 million tons of oil palm solid biomass by 2020 due to the increasing demand, which consists of empty fruit bunches, palm kernel shells (PKS), oil palm fronds, and mesocarp fibres [2]. At the same time, a considerable volume of solid biowaste is generated. Currently, the trend in conservation is to convert this solid biowaste into a valuable resource. Biomass processing enables the commercialization of bioenergy by-products using newly developed technologies [3].

Previous studies have demonstrated the presence of phenolics in palm oil seeds, fresh fruit bunches, fruit branches without fruits and leaves [4,5]. The economic viability of lignocellulosic biomass rich in palm kernel shells (PKS), oil palm fronds (OPF) and empty fruit bunches (EFB) is remarkable. Due to high lignin concentration, 70% of PKS consists of phenolic compounds [6,7]. Lignin has a saccharide structure composed of cellulose and hemicellulose. As the reaction temperature increases, lignin is degraded over a wide temperature range as the bonds (ether and carbon-carbon bonds) are gradually broken. The bond breaking between the monomer units results in the formation of significant amounts of phenolic compounds [8].

Vanillic acid has been reported to be a nutrient with antioxidant and antibacterial activity and a by-product of lignin degradation [9,10]. Its derivatives have significant functional uses as primary flavouring agents in the pharmaceutical, culinary, and cosmetic industries [11,12]. It has also been recovered from biomass and used in the food and pharmaceutical industries [13,14]. Membrane-based separation could be one of the most unique and distinctive approaches for downstream production of high-value goods in biorefineries. Membrane technology is gaining popularity because it is inexpensive, provides barriers to dissolved particles and pathogens, provides reliable filtration and adsorption processes, and is very easy to fabricate devices. This technique depends on binding and close association between ion exchange resins and the target molecule in solution to achieve high adsorption.

However, the limitation of these separation techniques has led to continued research into the most efficient technologies for lignocellulose recovery. The combination of adsorbent and membrane separation is considered the most effective mixed membrane technology. Mixed matrix membrane (MMM) usually involves the incorporation of nano- or micro-sized adsorbents into a polymer matrix to form porous adsorptive membranes. Moreover, the elution method is so modest that vanillic acid remains bound [15]. The presence of adsorption sites on the surface of a mixed matrix membrane containing hydroxyl and phosphate groups could lead to high purity of vanillic acid. Adsorptive membrane technology requires simpler equipment and safer procedures. This technology can increase the yield and adsorption capacity, reduce the production cost, and simplify the fabrication and scalability [16]. Therefore, a mixed matrix membrane adsorbent is considered the most effective and efficient approach for the recovery of vanillic acid.

Hydroxyapatite provides synergistic performance by combining the advantages of organic and inorganic elements [17]. The production of HAP from natural calcium resources such as bones, shells, corals, minerals, eggshells, and fish scales, among others, is a viable option to produce HAP because of its high calcium content. However, commercial hydroxyapatites are very expensive due to the high purity of their reagents [18]. On the other hand, HAP, which is derived from eggshells, exhibits these chemical properties, and can be prepared by simple and inexpensive methods. Common methods for the preparation of HAp include solid-state, hydrothermal, co-precipitation, sol-gel, and mechanochemical synthesis [19].

Vanillic acid is a natural compound found in fruits and vegetables that has antioxidant properties. Vanillic acid can interact with hydroxyapatite in several ways, including adhering to the surface, forming complexes with calcium ions, and altering the surface [20]. The exact details of this

interaction are determined by factors such as concentration, pH, temperature and time. Further research is needed to fully understand the interaction of hydroxyapatite and vanillic acid.

In this study, a functionalized mixed matrix membrane (MMM_{HAp}) with a bio-filler was prepared to enhance the recovery of vanillic acid from palm oil black liquor. The objective was to investigate whether the addition of hydroxyapatite (HAp) as a filler can improve the affinity and adsorption capacity of MMM for vanillic acid. It was hypothesized that modifying the existing MMM with HAp would improve its ability to separate vanillic acid by increasing its adsorption capacity for this compound. The optimal method for separating vanillic acid, including pH and initial concentration, was determined, and the physicochemical changes were evaluated using Fourier transform infrared spectroscopy (FTIR), scanning electron microscope (SEM), and X-ray diffraction (XRD). The results of this study pave the way for the synthesis and recovery of value-added products from biowaste and represent a significant achievement.

2. Methodology

2.1 Materials

Only analytical grade chemicals were used. Hydroxyapatites were prepared using 85% orthophosphoric acid (H_3PO_4)(Merck, Germany) as the phosphate source. Folin-Ciocalteu reagent (FC)(Sigma Aldrich, USA), vanillic acid (Sigma Aldrich, USA), anhydrous sodium carbonate (Na_2CO_3)(R&M Chemicals, UK), disodium hydrogen phosphate (Na_2HPO_4)(R&M Chemicals, UK), and disodium hydrogen phosphate dihydrate ($Na_2HPO_4.2H_2O$)(R&M Chemicals, UK) were purchased for MMM_{HAp} assay. Polyethersulfone pellets (PES) (MW=25000 g/mol, AMTEC, Universiti Teknologi Malaysia), polyvinylpyrrolidone (PVP) (MW=24000 g/mol, Sigma Aldrich, USA) and N-methyl-2-pyrrolidone (NMP)(Sigma Aldrich, USA) were used as pore-forming agent and solvent, respectively.

2.2 Preparation of Hydroxyapatite (HAp)

Eggshells were collected from bakery stores in the Kuala Terengganu region. First, the eggshells were cleaned and boiled in distilled water for 30 min to remove the eggshell membrane. Then, they were calcined in an oven at 100 °C for 60 min, and the temperature was raised to 900 °C for 3 h to recover the calcium oxide (CaO). Then, a wet chemical precipitation method was used to prepare HAp [21]. First, 79.6 g CaO from calcined eggshells was dissolved in 500 mL distilled water and stirred at 1000 rpm for 24 h. Then, 97.3 g of H_3PO_4 solution was added and stirred continuously for 24 h for the maturation phase. The mixture was maintained at pH 9 by the addition of NH_4OH solution. Then, the obtained white precipitate (hydroxyapatite) was filtered, purified and dried in an oven at 100 °C for 4 h. Subsequently, the hydroxyapatite was calcined in the furnace for 1 h at various temperatures from 100 °C to 800 °C and designated as HAp-ES100, HAp-ES200, HAp-ES300, HAp-ES400, HAp-ES500, HAp-ES600, HAp-ES700 and HAp-ES800, respectively.

2.3 Preparation of the Modified Mixed Matrix Membrane (MMM_{HAp})

The modified MMM_{HAp} dope solution was prepared, 74 g of NMP was heated to 60 ºC for 10 min, then 19 g of PES was added, and the solution was homogenized with constant stirring. Then 7 g of distilled water was added with a dropper. Finally, the heat was turned off, and 1 g of PVP was added dropwise, followed by 2 g of selected HAp. The solution was cooled to room temperature before degassing in a Schott flask to avoid defects in the casting solution [22]. The asymmetric flat sheet MMM_{HAp} film was fabricated using the dry/wet inversion method with a semi-automatic electric

casting machine with a 200 μm casting knife gap on the glass plate. The MMM$_{HAp}$ was washed with distilled water before being subjected to a water permeation test. Then, the MMM$_{HAp}$ was cut into a disk with an area of 0.00146 m^2 for the filtration setup and into rectangular shapes with a size of 2 mm x 1 mm and a weight of 0.015 g with an accuracy of ±0.001 using an electrical balance for further analysis.

2.4 Characterization of Hydroxyapatites (HAp) and Mixed Matrix Membranes (MMM$_{HAp}$)

Prior to characterization, HAp and MMM$_{HAp}$ were oven dried overnight at 70 ºC and ground to powder. For analysis at SEM, MMM$_{HAp}$ plates were cut into 1 cm x 1 cm pieces to represent the cross-sectional image. HAp and MMM$_{HAp}$ were examined for surface morphology analysis using a scanning electron microscope (SEM) (model JSM 63 80 LA) at 700x magnification and 10 kV under high vacuum conditions. Fourier transform infrared spectrophotometer with attenuated total reflectance (ATR-FTIR) (IRTRACE100, Shimadzu) using the KBr pellet technique at a ratio of (1:7) was used to identify the presence of the functional group of HAp and MMM$_{HAp}$. The purity of the HAp was also investigated by X-ray diffraction (XRD, Rigaku D/ MAX 2200/ PC Model).

2.5 Preparation of Black Liquor from Palm Kernel Shell (PKS)

The palm kernel shell (PKS) was extensively rinsed with distilled water and dried overnight at 100 °C in a vacuum oven. Then, 28 g of PKS was extracted using the Soxhlet extraction process with 400 ml anhydrous ethanol in a 500 ml round bottom flask and heated at 79°C using a heating mantle for 12 h. Next, the dark brown extraction solvent was filtered and dried using a rotary evaporator at 79°C until the solution turned black liquor. Then, the black liquor was transferred to a glass vial and chilled at -4 °C for two weeks before further use.

2.6 Performance test of Hydroxyapatite (HAp) on Vanillic Acid Adsorption

A batch adsorption study of vanillic acid was carried out to determine the best performance of hydroxyapatite (HAp) calcined at different temperatures. First, 0.1 g of HAp was added to a centrifuge tube, and 10 mL of 50 mg/L vanillic acid was added. The mixture was then shaken with a multirotator at 250 rpm. After 1 h, the eluent was tested using the Folin–Ciocaltue (FC) reagent method and evaluated at UV-VIS at 310 nm for detection of vanillic acid. All experiments were performed in triplicate. The adsorption capacity was calculated using the following equation:

$$q_e = (C_o - C_f)\frac{V}{m} \qquad (1)$$

Where q_e is the adsorption capacity (mg/g) of the adsorbent at equilibrium; C_o and C_f are the initial and final concentrations of the adsorbate in the solution (mg/L), V is the volume of the solution (L), and m is the mass of the adsorbent (g). The best performance of HAp was determined and selected for subsequent analysis. The percentage of adsorption was calculated as follows:

$$\% = \frac{C_i - C_f}{C_i} \times 100 \qquad (2)$$

C_i and C_f were the initial and final vanillic acid concentrations, respectively.

2.7 Performance test of MMM$_{Hap}$ on Vanillic Acid Adsorption
2.7.1 Effect on pH

The effect of pH conditions was studied at pH 3-8 to determine the optimum pH for adsorption of vanillic acid using a buffer solution. For pH 3-5, acetate buffer was used by mixing 15 ml of buffer solution with 0.015 g of MMM$_{HAp}$ membrane film and 0.005 g of vanillic acid powder, followed by stirring for 1 h at room temperature. Then, the eluent was quantified by the method Folin – Ciocaltue (FC) and repeated in triplicate. Finally, the adsorption capacity was calculated using Eq. (1). These procedures were repeated for pH6-pH8 (Table 1).

Table 1
Preparation of buffer solutions for vanillic acid adsorption study

Acetate buffer solutions			
pH	0.2 M acetic acid solution (mL)	0.2 M sodium acetate solution (mL)	Water (mL)
3.0	2.0	48.0	50
4.0	41.0	9.0	50
5.0	14.8	35.2	50
Phosphate buffer solution			
pH	Sodium phosphate, mono salt solution (mL)	Sodium phosphate, di-salt solution (mL)	Water (mL)
6.0	43.85	6.15	50
7.0	19.50	30.50	50
8.0	2.65	47.35	50

2.7.2 Effect on initial concentration

The concentration of vanillic acid (50-250 mg/l) was used to study the effect of the initial concentration of vanillic acid. The MMM$_{HAp}$ membrane was dried at 80°C in a vacuum oven before use. Then, 0.015 g of MMM$_{HAp}$ was added to 10 ml of vanillic acid solution in a 15 ml centrifuge tube and shaken at room temperature (25 °C) for 4 h. The percentage (%) of removal and the amount of adsorbent in the solid phase (mg/g) were calculated according to Eq. (1) and Eq. (2). These data are used for the analysis of the adsorption study.

2.8 Equilibrium Study of MMM$_{Hap}$ Adsorbent

In developing a biosorption system, the equilibrium adsorption isotherm is essential. The type of adsorption isotherms data shown can describe the interaction between the adsorbent and adsorbate in equilibrium. For the adsorption equilibrium study, the MMM$_{HAp}$ adsorbent was evaluated using equilibrium Langmuir and Freundlich's isotherm models to describe the adsorbent's adsorption, either homogenous or heterogeneous sorption. These models were used for vanillic acid adsorption onto MMM$_{HAp}$. The non-linear of Langmuir equation can be written as follows:

$$q_e = \frac{Q_{max} \cdot K_L \cdot C_e}{1 + K_L \cdot C_e} \tag{3}$$

Where can be represent in linear form,

$$\frac{1}{q_{eq}} = \frac{1}{q_m} + \frac{K_d}{q_m} \times \frac{1}{C_{eq}} \tag{4}$$

$$\frac{C_e}{q_e} = \frac{1}{(q_{max}k)} + \left(\frac{1}{q_{max}}\right) C_e \tag{5}$$

C_e is the equilibrium concentration of vanillic acid in solution (mg/L), q_e is the adsorbed vanillic acid concentration on the membrane adsorbent (mg/g), q_{max} is the maximum adsorption capacity (mg/g), and K_d is the dissociation constant of the adsorption rate. A plot of C_e/q_e versus C_e was plotted d to determine q_{max} and K_d as Langmuir isotherm's parameters using a linear curve fitting. From the value of K_d obtained from the graph, the equilibrium parameter, R_L, was calculated as follows.

$$R_L = \frac{1}{1 + K_L C_0} \tag{6}$$

Where,
C_0 = maximum initial concentration (mg/L)
K_d = Langmuir dissociation constant (L/mg)

The R_L value of the Langmuir isotherm shows the adsorption nature to be unfavorable ($R_L > 1$), linear ($R_L = 1$) and favorable ($0 < R_L < 1$). The Freundlich isotherm equation can be written in non-linear equation as stated below:

$$q_e = K_F C_e^{1/n} \tag{7}$$

And in linear equations as follows [23];

$$Lnq_e = \ln K_f + \left(\frac{1}{n}\right) \ln C_e \tag{8}$$

Where C_e is the equilibrium of vanillic acid concentration (mg/L), q_e is the equilibrium quantity of the vanillic acid adsorbed onto the membrane surfaces (mg/L), and n is the Freundlich constant, which corresponds to the affinity of ion absorbed onto the surface of the membranes, and K_f is the Freundlich dissociation constant. A plot of ln q_e and ln C_e was plotted to find the value of n and K_f from the slope and intercept of the plot, respectively.

2.9 Kinetic Study of MMM_{HAp} Adsorbent

The study of kinetic models is necessary to identify the mechanism involved in the adsorption of adsorbate onto adsorbent in an aqueous solution, as well as its possible rate-controlling processes, such as mass transport and the chemical reaction process. It may be calculated by fitting the experimental data to McKay's and Ho's pseudo-first-order and pseudo-second-order kinetic models, respectively [24]. A simple kinetic analysis of adsorption is the pseudo-first-order equation in non-linear form;

$$\frac{dq}{dt} = k_1 \cdot (q_e - q_t) \tag{9}$$

Where q_e, the equilibrium quantity of lead adsorbed by the adsorbent and q_t, the specific time (mg/g). The integration of Eq. (9) represents the linear of pseudo-first equation is denoted by the following equation [25]:

$$\log(q_e - q_t) = \log q_e - \frac{K_1 t}{2.303} \tag{10}$$

The biosorption rate constant of pseudo-first-order sorption is K_1 (1/min). The pseudo-first-order graph was displayed as a log $(q_e - q_t)$ against t . K_1 is the slope of the graph, whereas q_e, the intercept-y. In addition, a pseudo-second-order equation based on adsorption capacity is shown in Eq. (11).

$$\frac{dq_t}{dt} = k_s \cdot (q_e - q_t)^2 \tag{11}$$

And, in linear equation of the pseudo-second-order model is given below:

$$\frac{t}{q_t} = \frac{1}{k_2 q_e^2} + \frac{1}{q_e} t \tag{12}$$

Where, the rate is constant, k_2 (g/mg min), and q_e are calculated from the intercept and slope of a pseudo-second-order linear curve plotted t/qt versus t. The initial biosorption rate, h, can alternatively be calculated using the equation above and the $k_2 q_e^2$ formula.

2.10 Performance of Mixed Matrix Membrane (MMM$_{HAp}$) Modified Adsorbent for Vanillic Acid Separation from Real Wastes of Palm Kernel Shells (PKS)

0.015 g of MMM$_{HAp}$ was put in 10 mL black liquor solutions with a 500x dilution factor. Following the previous procedure, the vanillic acid was analyzed at intervals using the UV-Vis spectrophotometer at 310 nm wavelength. All the experiments were repeated in triplicate. The performance of MMM$_{HAp}$ was determined by evaluating the adsorption capacity using Eq. (1) and Eq. (2).

3. Results
3.1 Characterization of Hydroxyapatite (HAp) Recovered from the Eggshell Effect of Calcination Temperature
3.1.1 Morphology of HAp at different temperature

Figure 1 shows the SEM micrographs of HAP powders prepared by wet chemical precipitation at various calcination temperatures [26]. Hydroxyapatite was present as relatively uniform fine particles that were slightly agglomerated and cold welded. The aggregates were rough, granular to dense, and their particles had different shapes such as short and long columns.

All HAp nanoparticles had irregular morphology and small rod-shaped crystals with size less than 100 nm. The microstructure consisted of small pores that were constantly present at the grain boundaries. The morphology of hydroxyapatite crystals varied as a function of calcination temperature [27]. Agglomeration was observed at HAP with increasing calcination temperature [28]. The images from SEM show the cross-linked HAp particles in voluminous form. The initial nanocrystals have grown together (Figure 1 (a)), and the presence of additional porosity caused by crystal development can be seen (Figure 1(b) to Figure 1(h)), but the porosity within the nanocrystals remains.
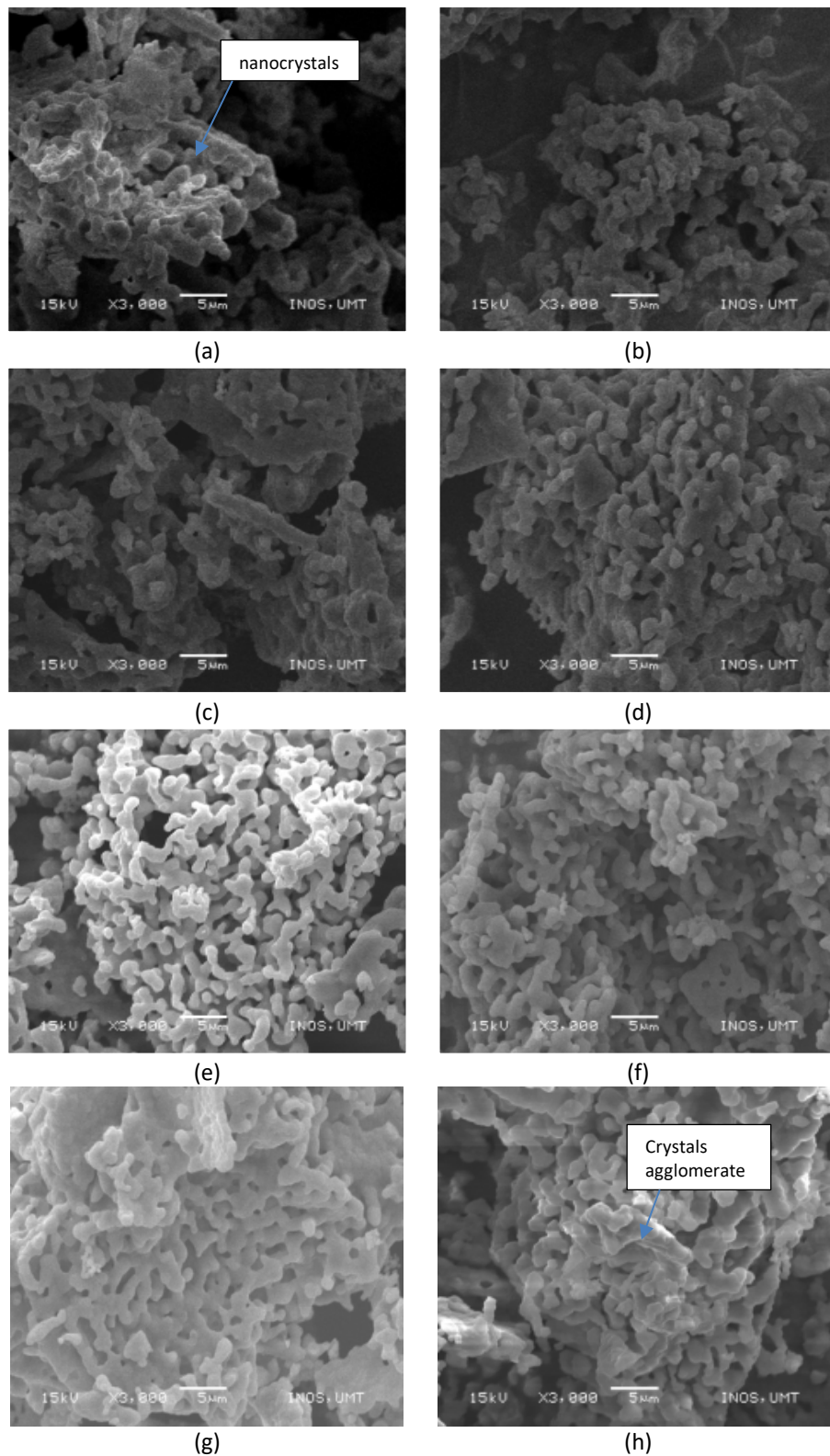
Fig. 1. SEM micrographs for HAp at different calcination temperature; (a) 100 °C, (b) 200 °C, (c) 300 °C, (d) 400 °C, (e) 500 °C, (f) 600 °C, (g) 700 °C, and (h) 800 °C

The images from SEM show that the crystal particles agglomerated with increasing calcination temperature [29,30]. Crystal growth was initiated by the process of nucleation, aggregation and agglomeration [31]. The aggregation of elemental nanocrystals is driven by various nanometer/colloid-scale forces that promote the reduction of surface free energy [32].

3.1.2 Fourier Transform Infrared (FTIR) of hap from eggshell

The formation of HAP was further characterized by FTIR analysis. Figure 2 presents FTIR spectra of HAP powders after wet chemical precipitation process at different calcination temperatures which is 100 °C to 800 °C. The representative FTIR spectrum shows all adsorption peaks of HAP synthesized from eggshells. FTIR tested for the presence of functional groups such as carbonate (CO_3^{2-}), phosphate $(PO_4)_3^{2-}$ and hydroxyl (OH) which accounts for the presence of hydroxyapatite.
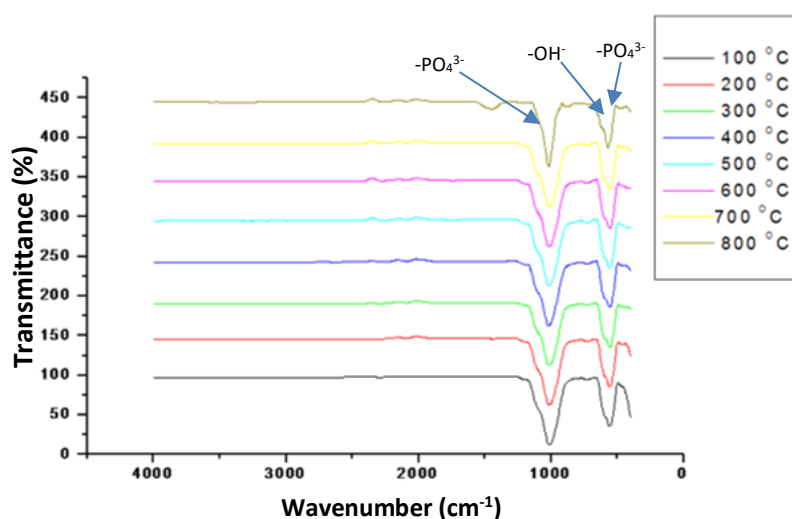

Fig. 2. The FT-IR spectra of HAp calcined at (a) 100 °C, (b) 200 °C, (c) 300 °C, (d) 400 °C, (e) 500 °C, (f) 600 °C, (g) 700 °C, and (h) 800 °C

FTIR analysis of HAP spectra reveals the presence of phosphate ($-PO_4^{3-}$) and hydroxyl ($-OH^-$) peaks characteristic of HAp compounds (Figure 2). A medium-sharp peak at 650 cm^{-1} indicates the hydroxyl (O-H) bending deformation mode [33]. This peak of O-H bands embodying adsorbed water starts to disappear when the calcination temperature increases to 800 °C. The P-O vibrations of the bending and stretching modes appear at 554 cm^{-1} and 1031 cm^{-1}, respectively [34]. The weak carbonate peak (CO_3^{2-}) at a wavelength of 1465 cm^{-1} suggests that the PO_4^{3-} substituted by the carbonate group may be due to the interaction of calcite and carbon dioxide at high temperatures (800°) [35]. Under certain conditions, the carbonated compound enhanced the bioactivity of HAp [36].

3.1.3 X-Ray diffraction of HAp

The effect of calcination temperatures on the crystallinity of the powders of HAP was studied in detail using XRD analysis. The obtained XRD peaks (Figure 3) were consistent with the conventional hydroxyapatite peaks (HAP).
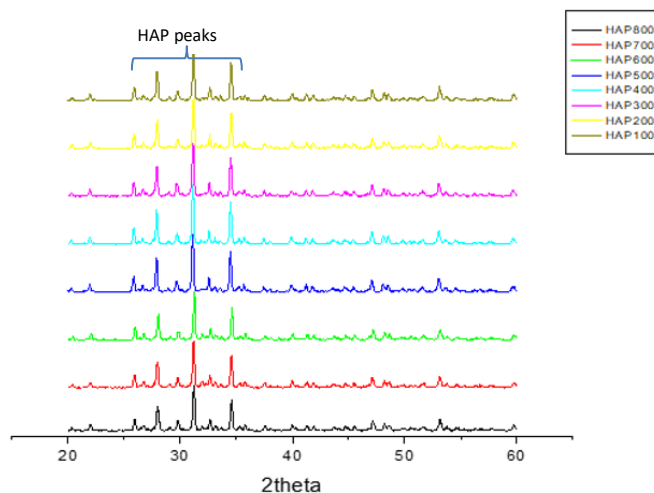
Fig. 3. X-ray diffraction patterns of hydroxyapatite synthesized with different temperatures ranging from 100 °C – 800 °C

It indicated the successful formation of hydroxyapatite according to the International Centre for Diffraction Data (JSDS No. 09-0432), as shown at $2\theta=25°$ to $34°$ [37]. The peaks at 2θ from $26°$ to $34°$ become narrower when HAP is calcined at high temperatures. The broad XRD spectra show the fraction of amorphous phase at low temperatures in the calcination phase (100 °C to 300 °C). The XRD patterns of HAp calcined at 600 °C show high shaper peaks, demonstrating the high crystallinity [38]. When the temperature increases from 500 °C to 800 °C, the peaks become narrower, indicating the highly crystalline phase, and fixing the sintering temperature improves the production of crystalline HAp powder [39,40]. However, from the XRD analysis, the presence of a weak carbonate peak in the FTIR does not affect the purity of the HAp produced.

3.2 Selection of Eggshell-Derived Hydroxyapatite (HAP): The Effect of Calcination Temperatures on Adsorption of Vanillic Acid

In this section, the performance of hydroxyapatites (HAp) calcined at different temperatures for the adsorption of vanillic acid, as shown in Figure 4. The results show that the trend of increasing the vanillic acid adsorption capacity of HAp calcined at temperatures between 100°C and 500°C was reversed when the calcination temperature was increased to 800°C.
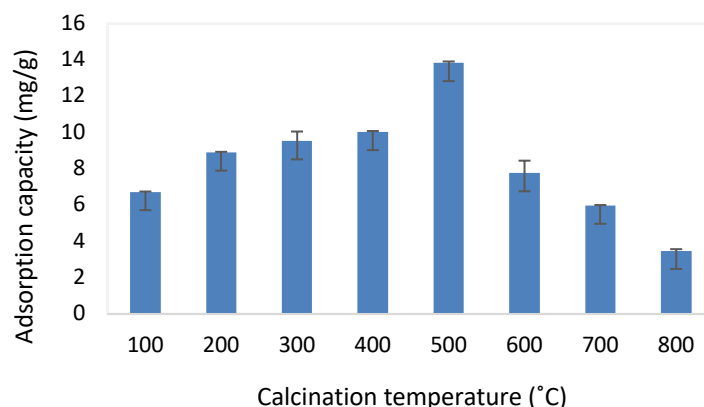

Fig. 4. The adsorption capacity of vanillic acid by hydroxyapatites calcined at different temperatures

The effect of calcination temperature resulted in different crystallinity, porosity, surface area and purity of HAp [41]. HAp calcined at 500°C showed the best performance, as it had a large active site surface area. This is consistent with a previous study which showed that HAp prepared at high calcination temperatures caused lower absorption of fluoride ions [42]. Another study showed that the tetrahedral (Td) structure of the dehydroxylate and the structure of the Pd^{2+}-containing species changed to a square-planar geometry (D4h) with increasing calcination temperature [43]. HAp calcined at 600 °C for 5 hours improved the quality of bovine bone-derived hydroxyapatite in the manufacture of wound dressings and implantable materials (BB-HAP) [44].

The adsorption tendency implies the active functional group between sorbent and adsorbent. In this study, HAp calcined at 500 °C was shown to have the best physical properties for adsorption of vanillic acid and was selected as a filler to improve mixed matrix membrane (MMM_{HAp}). These results demonstrate the importance of optimizing the calcination temperature of HAp to improve its performance for specific applications, such as the recovery of valuable compounds from biowaste.

3.3 Adsorption Vanillic Acid between Native Membrane (PES) and PES-Hap Membrane (MMM_{HAp})

Two different types of membrane have been discovered the adsorption of the vanillic acid. Figure 5 showed the removal percentage of vanillic acid form simulated water by using two different types of mixed matrix membranes in finding the selected membrane to be used for this study.
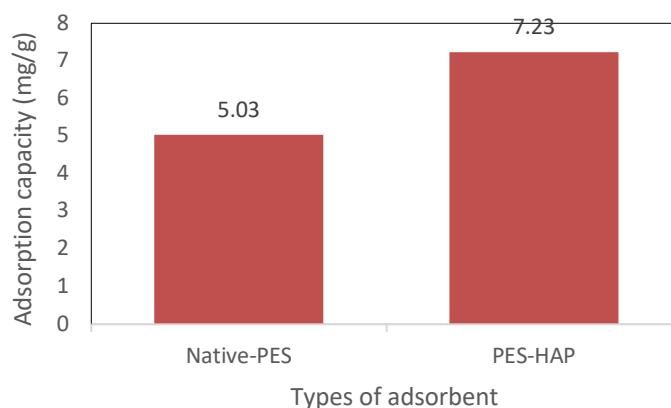

Fig. 5. Graph of adsorption capacity versus different mixed matrix membranes sample

Figure 5 showed modified membrane have higher adsorption capacity compared to native membrane. PES–HAP or MMM_{HAp} showed the highest adsorption capacity which was 7.23mg/g. This is show that HAP can improved the adsorption efficiency. Thus, PES–HAP or MMM_{HAp} membrane was selected as the best membrane to be used next.

3.4 Characterization Morphology of Native PES Membrane and PES-HAP Membrane

To observe the differences in the pore structures with and without the addition of hydroxyapatite (Hap), the morphology of the membrane cross-section was analyzed. As shown in Figure 6, the cross-sectional images of both membrane types show asymmetric structures with a dense skin layer, a porous intermediate layer, and macropores at the bottom.
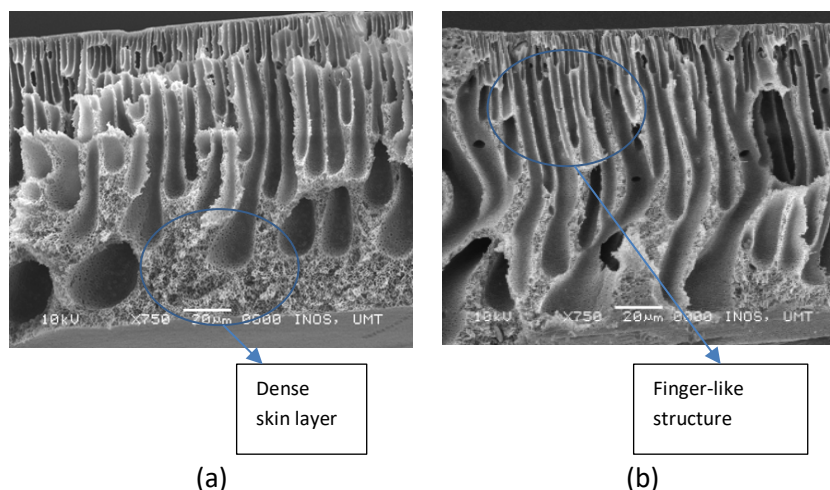
Fig. 6. Morphology cross section membrane; (a) native membrane (PES), (b) PES-Hap (MMM$_{HAp}$)

However, a significant difference between the native polyethersulfone membrane (PES) and the PES -HAp membrane is that the finger-like structures of the modified membrane are much smaller than those of the native membrane. In addition, the finger-like structures in the modified membrane are more elongated and more connected to the porous layer. This could be due to the successful incorporation of hydroxyapatite nanoparticles into the membrane. The accumulation of hydroxyapatite in certain areas of the membrane, especially in the finger-like structures and the porous layers, indicates that the Hap nanoparticles were effectively integrated. It is worth noting that Hap naturally exists in the form of aggregates, which could explain the observed agglomeration.

In the native membrane, the finger-like structures were larger and formed a sponge-like structure, probably due to the rapid precipitation during the phase inversion process. The strong interaction of hydroxyl groups (O-H) in the membrane also contributed to the formation of the sponge-like structure. The active layer of the modified membrane was denser than that of the native membrane, which may indicate improved performance. Overall, the results suggest that the addition of Hap nanoparticles could improve the morphology and performance of the membrane PES.

3.5 Determination of pH-Medium Conditions for Modified Mixed Matrix Membranes (MMM$_{HAp}$)

The adsorption of vanillic acid by modified MMM$_{HAp}$ was studied in a medium with acidic to alkaline pH (Figure 7). The study showed that the maximum adsorption of vanillic acid occurred at pH 8, which is slightly alkaline. The reason for this high adsorption capacity was attributed to the modified configuration of vanillic acid, which increased the chemical interaction with the active sites of MMM$_{HAp}$. Vanillic acid tends to ionize and increase its ionic strength under alkaline conditions, which enhances the electrostatic interaction and adsorption on HAp adsorbents. The increase in ionic strength of vanillic acid under alkaline conditions also leads to a stronger attraction between the positively charged HAp surface and the negatively charged vanillic acid molecules, promoting adsorption [45]. The pH influences not only the active sites on the biosorption surface, but also the properties of the adsorbed ions [46]. When the pH of the medium changes, the availability of H$^+$ ions decrease, which affects the chemical interactions between the solution and the sorbent and leads to a change in the properties of the adsorbed ions.
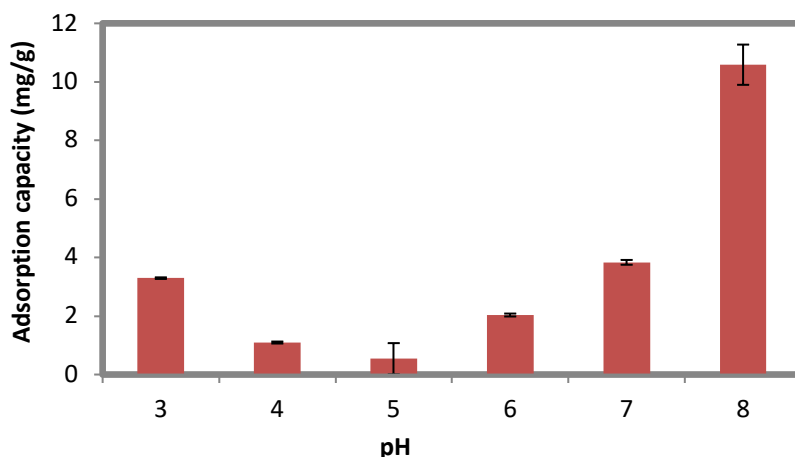
Fig. 7. The adsorption capacity of MMM$_{HAp}$ for vanillic acid versus pH

In an acidic medium, the interaction between vanillic acid and the MMM$_{HAp}$ surface is low due to the competitive adsorption between the predominantly available H$^+$ and vanillic acid at the active site. However, when the pH of the medium increased to a natural and alkaline range, the maximum adsorption capacity of vanillic acid increased. This indicates that the pH of the medium plays a crucial role in determining the efficiency of the adsorption process [47]. Therefore, for the following analysis of MMM$_{HAp}$, pH 8 was used as the most favorable pH medium for the adsorption of vanillic acid onto MMM$_{HAp}$. This is because the maximum adsorption of vanillic acid was observed at pH 8, indicating that the chemical interaction between vanillic acid and MMM$_{HAp}$ surface was most efficient. This information is important for the optimization of the adsorption process for the removal of vanillic acid with MMM$_{HAp}$.

3.6 Effect of Different Initial Concentrations on Adsorption of Vanillic Acid on MMM$_{HAp}$

Figure 8 shows the effect of different initial concentrations on the adsorption capacity of vanillic acid for 240 min. Adsorption is the process of attaching molecules, ions or particles to a surface and is a common method of removing impurities from aqueous solutions. The figure shows that the adsorption capacity of vanillic acid increases rapidly within the first 15 min of contact with MMM$_{HAp}$ surfaces. It remained constant as the optimum duration approached 60 min and then 240 min. This phenomenon can be explained by the availability of active sites on the MMM$_{HAp}$ surfaces for the attachment of vanillic acid. The active sites refer to the vacant sites on the surface to which the vanillic acid molecules can bind via various mechanisms such as hydrogen bonding, electrostatic interactions, or van der Waals forces. The MMM$_{HAp}$ adsorbent has a large surface area and inter- or intra-nanofibrous pores, which provide a large number of active sites for vanillic acid binding, as reported in the literature [48].
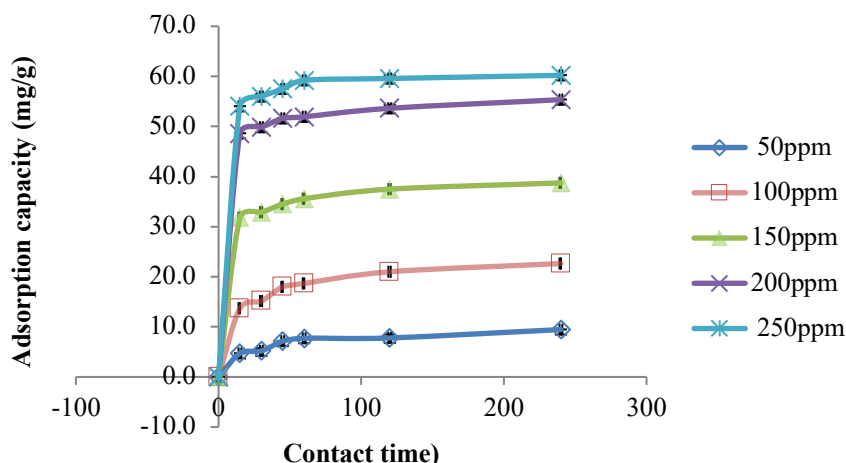
Fig. 8. Effects of different initial concentrations and contact times on the adsorption capacity of vanillic acid using pH 8

As the contact time between MMM$_{HAp}$ surfaces and vanillic acid molecules increases, the adsorption capacity of vanillic acid reaches a plateau. This plateau signifies the equilibrium state where the adsorption rate equals the desorption rate of vanillic acid molecules from the active sites of the surface. At this point, the surface sites are saturated with vanillic acid molecules, and no further adsorption can occur. In this study, the maximum adsorption capacity of the MMM$_{HAp}$ adsorbent was found to be 60.2 mg/g, and equilibrium was reached within 60 min of contact time [49].

3.7 Equilibrium and Kinetic Adsorption Study of Vanillic Acid on an Improved Mixed Membrane Adsorbent (MMM$_{HAp}$)

The evaluation of sorption mechanisms was based on the Langmuir and Freundlich isotherm models (Figure 9). The Freundlich isotherm model provided a better fit to the experimental data, as evidenced by the higher regression value (R^2) of 0.9999. In contrast, the Langmuir isotherm model proved to be inadequate for describing the adsorption process, as indicated by the negative value of q$_{max}$ from the Langmuir isotherm equation as stated in Table 2.
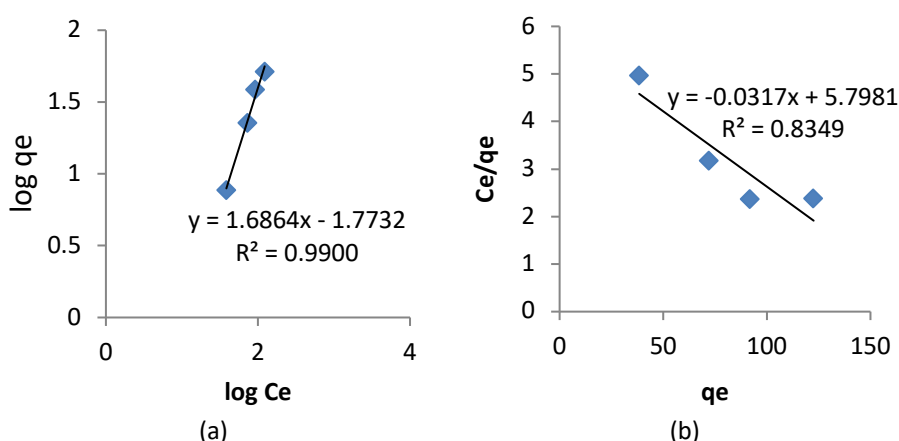

(a)   (b)

Fig. 9. The adsorption of vanillic acid onto PES/HAP MMMs plotted based on (a) Freundlich isotherm and (b) Langmuir isotherm models

Table 2
The Langmuir and Freundlich parameters of vanillic acid adsorption onto PES/HAP MMMs

Phenolic compound	Freundlich constants			Langmuir constants			
	R^2	K_F	n	R^2	q_{max} (mg/g)	K_L	R_L
Vanillic acid	0.9900	0.067	0.593	0.8349	-31.546	-0.0055	1.2658

The Freundlich isotherm model defines adsorption as a phenomenon occurring on heterogeneous surfaces by a multilayer adsorption process, and their energies are exponentially distributed [50]. The stronger binding sites are occupied first, and the adsorption energy decreases exponentially when the adsorption process is completed. The n value refers to the adsorption intensity of the adsorbate on the heterogeneous surface of the MMM_{HAp} adsorbent. The value of n ranges between 0<n<1 indicates a favourable adsorption isotherm [51], and a less intense value indicates a heterogeneous binding type [52].

As shown in Figure 10, the data from the vanillic acid adsorption experiment were well fitted to the pseudo-second order, with a higher R^2 of 0.9992 compared to the pseudo-first order (R^2 =0.6717). This result is consistent with the value of q_e (39.22 mg/L) and close to the experimental qe value (38.74 mg/L), as shown in Table 3. This model defined the chemisorption mechanism between vanillic acid and adsorbent surfaces and proposed the adsorption process as the rate-limiting step of the reaction [53]. It also described a sharing or exchange of electrons with activation energy [54].
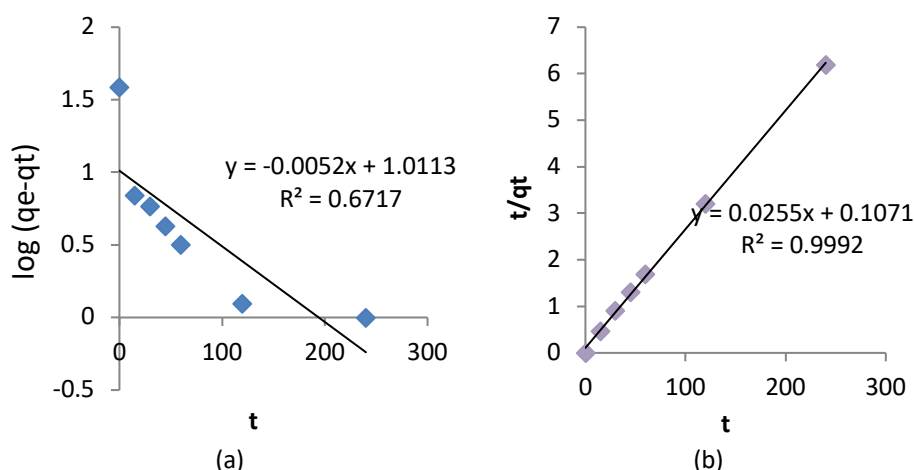

Fig. 10. The kinetic adsorption study of (a) pseudo-first-order and (b) pseudo-second-order for vanillic adsorption onto MMM_{HAp}

Table 3
Kinetic parameters for vanillic acid adsorption study onto MMM_{Hap}

q_e exp	Pseudo-first-order			Pseudo-second-order		
	R^2	K_1	q_e	R^2	K_2	q_e
38.74	0.6717	0.01198	10.26	0.9992	0.00607	39.22

3.8 Application of MMM_{HAp} for Vanillic Acid Recovery in Palm Oil Black Liquor

The result showed that the modified MMM_{HAp} exhibited high active vanillic acid adsorption in the complex structure of the real sample and reached the highest adsorption capacity of 170.8 mg/g. The percentage recovery of vanillic acid from palm oil black liquor was 60.9%. The enormous capacity of MMM_{HAp} to adsorb vanillic acid in the real sample compared to the synthetic solution was reflected in the presence of other phenolic compounds in the crude solution, which activated the active site of

MMM$_{HAp}$ and increased the adsorption capacity [55]. Moreover, the addition of HAp as a filler in MMM$_{HAp}$ could be a reliable approach to improve the efficiency of the adsorbent and is expected to be a promising approach for vanillic acid recovery in biomedical applications.

4. Conclusions

The use of eggshells as calcium precursors for hydroxyapatite formation and their subsequent incorporation as a filler in a mixed matrix membrane (MMM$_{HAp}$) has proven to be a successful approach to improve the recovery of vanillic acid from biowaste and palm oil black liquor. Calcination temperature plays a crucial role in determining the structural properties of HAp, and the study found that 500 °C is the optimal temperature for the preparation of HAp with suitable properties for vanillic acid adsorption. The high adsorption capacity of MMM$_{HAp}$ in the multisystem indicates that it is a promising adsorbent for the recovery of significant amounts of vanillic acid from biowaste, especially from palm kernel shells. These results highlight the commercial and industrial potential of MMM$_{HAp}$ and provide valuable insights to optimize its application for the recovery of valuable compounds in the pharmaceutical, chemical and food industries. This research highlights the importance of a green circular economy approach to generate income through resource recovery. Overall, the use of MMM$_{HAp}$ as an effective adsorbent for vanillic acid recovery contributes to the sustainability of our environment and economy.

References
[1] Zeb, Alam. "A comprehensive review on different classes of polyphenolic compounds present in edible oils." *Food Research International* 143 (2021): 110312. https://doi.org/10.1016/j.foodres.2021.110312
[2] Mohd Hamzah, Mohd Amir Asyraf, Rosnani Hasham, Nik Ahmad Nizam Nik Malek, Raja Safazliana Raja Sulong, Maizatulakmal Yahayu, Fazira Ilyana Abdul Razak, and Zainul Akmar Zakaria. "Structural-based analysis of antibacterial activities of acid condensate from palm kernel shell." *Biomass Conversion and Biorefinery* 13, no. 5 (2023): 4241-4253. https://doi.org/10.1007/s13399-021-02219-w
[3] Ilham, Zul, Nur Aida Izzaty Saad, Wan Abd Al Qadr Imad Wan, and Adi Ainurzaman Jamaludin. "Multi-criteria decision analysis for evaluation of potential renewable energy resources in Malaysia." *Progress in Energy and Environment* 21 (2022): 8-18. https://doi.org/10.37934/progee.21.1.818
[4] Abdullah, Fadzlina, and Nur Aainaa Syahirah Ramli. "Identification of hydrophilic phenolic compounds derived from palm oil products." *Journal of Oil Palm Research* 32, no. 2 (2020): 258-270. https://doi.org/10.21894/jopr.2020.0020
[5] Kawamura, Fumio, Nur Syahirah Saary, Rokiah Hashim, Othman Sulaiman, Koh Hashida, Yuichiro Otsuka, Masaya Nakamura, and Seiji Ohara. "Subcritical water extraction of low-molecular-weight phenolic compounds from oil palm biomass." *Japan Agricultural Research Quarterly: JARQ* 48, no. 3 (2014): 355-362. https://doi.org/10.6090/jarq.48.355
[6] Choi, Gyung-Goo, Seung-Jin Oh, Soon-Jang Lee, and Joo-Sik Kim. "Production of bio-based phenolic resin and activated carbon from bio-oil and biochar derived from fast pyrolysis of palm kernel shells." *Bioresource Technology* 178 (2015): 99-107. https://doi.org/10.1016/j.biortech.2014.08.053
[7] Wannid, Prapudsorn, Bongkot Hararak, Sirada Padee, Wattana Klinsukhon, Natthaphop Suwannamek, Marisa Raita, Krit Khao-on, and Chureerat Prahsarn. "Structural and Thermal Characteristics of Novel Organosolv Lignins Extracted from Thai Biomass Residues: A Guide for Processing." *Journal of Polymers and the Environment* 30, no. 7 (2022): 2739-2750. https://doi.org/10.1007/s10924-022-02387-4
[8] Barontini, Federica, Enrico Biagini, and Leonardo Tognotti. "Influence of torrefaction on biomass devolatilization." *ACS Omega* 6, no. 31 (2021): 20264-20278. https://doi.org/10.1021/acsomega.1c02141

[9]   Abd-Aziz, Suraini, Mohd Azwan Jenol, and Illy Kamaliah Ramle. "Biovanillin from Oil Palm Biomass." *Biorefinery of Oil Producing Plants for Value-Added Products* 2 (2022): 493-514. https://doi.org/10.1002/9783527830756.ch25

[10]   Bhat, Rajeev, Aziz Ahmad, and Ivi Jõudu. "Applications of lignin in the agri-food industry." *Lignin: Biosynthesis and Transformation for Industrial Applications* (2020): 275-298. https://doi.org/10.1007/978-3-030-40663-9_10

[11]   Sharma, Neha, Nishtha Tiwari, Manish Vyas, Navneet Khurana, Arunachalam Muthuraman, and Puneet Utreja. "An overview of therapeutic effects of vanillic acid." *Plant Arch* 20, no. 2 (2020): 3053-3059.

[12]   Salau, Veronica F., Ochuko L. Erukainure, Collins U. Ibeji, Tosin A. Olasehinde, Neil A. Koorbanally, and Md Shahidul Islam. "Vanillin and vanillic acid modulate antioxidant defense system via amelioration of metabolic complications linked to Fe^{2+}-induced brain tissues damage." *Metabolic Brain Disease* 35 (2020): 727-738. https://doi.org/10.1007/s11011-020-00545-y

[13]   Khanam, Mehrun Nisha, Mohammad Anis, Saad Bin Javed, Javad Mottaghipisheh, and Dezső Csupor. "Adventitious root culture-An alternative strategy for secondary metabolite production: A review." *Agronomy* 12, no. 5 (2022): 1178. https://doi.org/10.3390/agronomy12051178

[14]   Jareonsin, Surumpa, and Chayakorn Pumas. "Advantages of heterotrophic microalgae as a host for phytochemicals production." *Frontiers in Bioengineering and Biotechnology* 9 (2021): 628597. https://doi.org/10.3389/fbioe.2021.628597

[15]   Khan, M. Kamran, Jianquan Luo, Rashid Khan, Jinxin Fan, and Yinhua Wan. "Facile and green fabrication of cation exchange membrane adsorber with unprecedented adsorption capacity for protein purification." *Journal of Chromatography A* 1521 (2017): 19-26. https://doi.org/10.1016/j.chroma.2017.09.031

[16]   Al-Shaeli, Muayad, Raed A. Al-Juboori, Saif Al Aani, Bradley P. Ladewig, and Nidal Hilal. "Natural and recycled materials for sustainable membrane modification: Recent trends and prospects." *Science of the Total Environment* 838 (2022): 156014. https://doi.org/10.1016/j.scitotenv.2022.156014

[17]   Oprea, Madalina, and Stefan Ioan Voicu. "Recent advances in applications of cellulose derivatives-based composite membranes with hydroxyapatite." *Materials* 13, no. 11 (2020): 2481. https://doi.org/10.3390/ma13112481

[18]   Cahyaningrum, S. E., N. Herdyastuty, B. Devina, and D. Supangat. "Synthesis and characterization of hydroxyapatite powder by wet precipitation method." In *IOP Conference Series: Materials Science and Engineering*, vol. 299, p. 012039. IOP Publishing, 2018. https://doi.org/10.1088/1757-899X/299/1/012039

[19]   Osseni, Sèmiyou, Etienne V. Sagbo, Raoul Ahouansou, Marielle y Agbahoungbata, David Neumeyer, Marc Verelst, and Robert Mauricot. "Synthesis of calcium phosphate bioceramics based on snail shells: towards a valorization of snail shells from Republic of Benin." *American Journal of Chemistry* 8 (2018): 90-95.

[20]   DileepKumar, V. G., Mysore Santosh Sridhar, Pornanong Aramwit, Valentina K. Krut'ko, Olga N. Musskaya, Ilya E. Glazov, and Narendra Reddy. "A review on the synthesis and properties of hydroxyapatite for biomedical applications." *Journal of Biomaterials Science, Polymer Edition* 33, no. 2 (2022): 229-261. https://doi.org/10.1080/09205063.2021.1980985

[21]   Alias, Maslinda, Sofiah Hamzah, Jasnizat Saidin, Norhafiza Ilyana Yatim, Mohammad Hakim Che Harun, Wan Anwar Fahmi Wan Mohamad, Nur Hanis Hayati Hairom, Asmadi Ali, and Nora'aini Ali. "Integration of hydroxyapatite from fish scales and polyethersulfone membrane for protease separation from Bacillus subtilis." *Separation Science and Technology* 57, no. 6 (2022): 910-928. https://doi.org/10.1080/01496395.2021.1948866

[22]   Yogarathinam, Lukka Thuyavan, Pei Sean Goh, Ahmad Fauzi Ismail, Arthanareeswaran Gangasalam, Nor Akalili Ahmad, Alireza Samavati, Stanley Chinedu Mamah, Muhammad Nidzhom Zainol Abidin, Be Cheer Ng, and Balamurugan Gopal. "Nanocrystalline cellulose incorporated biopolymer tailored polyethersulfone mixed matrix membranes for efficient treatment of produced water." *Chemosphere* 293 (2022): 133561. https://doi.org/10.1016/j.chemosphere.2022.133561

[23]   Sharma, Dilip K., Fengting Li, and Yi-nan Wu. "Electrospinning of Nafion and polyvinyl alcohol into nanofiber membranes: A facile approach to fabricate functional adsorbent for heavy metals." *Colloids and Surfaces A: Physicochemical and Engineering Aspects* 457 (2014): 236-243. https://doi.org/10.1016/j.colsurfa.2014.05.038

[24]   Revellame, Emmanuel D., Dhan Lord Fortela, Wayne Sharp, Rafael Hernandez, and Mark E. Zappi. "Adsorption kinetic modeling using pseudo-first order and pseudo-second order rate laws: A review." *Cleaner Engineering and Technology* 1 (2020): 100032. https://doi.org/10.1016/j.clet.2020.100032

[25]   Yatim, Norhafiza Ilyana, Marinah Mohd Ariffin, and Sofiah Hamzah. "Removal of heavy metals using self-integrating bio-adsorbent from agricultural by-products and marine waste materials." *Desalination and Water Treatment* 118, no. 1 (2018): 216-229. https://doi.org/10.5004/dwt.2018.22622

[26]   Cheah, Kingsly Tian Chee, and Jing Yao Sum. "Synthesis and evaluation of Fe-doped zinc oxide photocatalyst for methylene blue and congo red removal." *Progress in Energy and Environment* 22 (2022): 13-28. https://doi.org/10.37934/progee.22.1.1328

[27] Hasan, Mohamad Rais, Norfatin Syazani Mohd Yasin, and Mohd Sabri Mohd. "Proximate and morphological characteristics of nano hydroxyapatite (Nano HAp) extracted from fishbone." *Journal of Sustainability Science and Management* 15, no. 8 (2020): 9-21. https://doi.org/10.46754/jssm.2020.12.002

[28] Agbabiaka, O. G., I. O. Oladele, A. D. Akinwekomi, A. A. Adediran, Ayokunle O. Balogun, O. G. Olasunkanm, and T. M. A. Olayanju. "Effect of calcination temperature on hydroxyapatite developed from waste poultry eggshell." *Scientific African* 8 (2020): e00452. https://doi.org/10.1016/j.sciaf.2020.e00452

[29] Zubieta-Otero, Luis F., Sandra M. Londoño-Restrepo, Gilberto Lopez-Chavez, Ezequiel Hernandez-Becerra, and Mario E. Rodriguez-Garcia. "Comparative study of physicochemical properties of bio-hydroxyapatite with commercial samples." *Materials Chemistry and Physics* 259 (2021): 124201. https://doi.org/10.1016/j.matchemphys.2020.124201

[30] Obada, D. O., E. T. Dauda, J. K. Abifarin, D. Dodoo-Arhin, and N. D. Bansod. "Mechanical properties of natural hydroxyapatite using low cold compaction pressure: Effect of sintering temperature." *Materials Chemistry and Physics* 239 (2020): 122099. https://doi.org/10.1016/j.matchemphys.2019.122099

[31] Tourbin, Mallorie, Fabien Brouillet, Basile Galey, Nicole Rouquet, Pierre Gras, Nicolas Abi Chebel, David Grossin, and Christine Frances. "Agglomeration of stoichiometric hydroxyapatite: Impact on particle size distribution and purity in the precipitation and maturation steps." *Powder Technology* 360 (2020): 977-988. https://doi.org/10.1016/j.powtec.2019.10.050

[32] Kumar, C., D. Kaliyan, Ramasamy Mariappan Vimalathithan, Perumal Ilaiyaraja, and S. Govindhasamy. "Structural, morphological and anti-bacterial analysis of nanohydroxyapatite derived from biogenic (SHELL) and chemical source: formation of apatite." *Iranian Journal of Materials Science and Engineering* 18, no. 1 (2021): 91-109.

[33] Khan, Haris Mahmood, Tanveer Iqbal, Chaudhry Haider Ali, Saima Yasin, and Farrukh Jamil. "Waste quail beaks as renewable source for synthesizing novel catalysts for biodiesel production." *Renewable Energy* 154 (2020): 1035-1043. https://doi.org/10.1016/j.renene.2020.03.079

[34] Sánchez-Campos, Daniel, Maria Isabel Reyes Valderrama, Susana López-Ortíz, Daniela Salado-Leza, María Eufemia Fernández-García, Demetrio Mendoza-Anaya, Eleazar Salinas-Rodríguez, and Ventura Rodríguez-Lugo. "Modulated monoclinic hydroxyapatite: The effect of pH in the microwave assisted method." *Minerals* 11, no. 3 (2021): 314. https://doi.org/10.3390/min11030314

[35] Syafaat, Firda Yanuar, and Yusril Yusuf. "Effect of Ca: P concentration and calcination temperature on hydroxyapatite (HAp) powders from quail eggshell (Coturnix Coturnix)." *International Journal of Nanoelectronics and Materials* 11 (2018): 51-58.

[36] Jiang, Xiaodan, Yi Zhao, Chen Wang, Ruixue Sun, and Yuanzheng Tang. "Effects of physico-chemical properties of ions-doped hydroxyapatite on adsorption and release performance of doxorubicin as a model anticancer drug." *Materials Chemistry and Physics* 276 (2022): 125440. https://doi.org/10.1016/j.matchemphys.2021.125440

[37] Liu, Yu-Cheng, Ying-Te Lee, Tse-Chiang Huang, Geng-Sheng Lin, Yi-Wen Chen, Bor-Shiunn Lee, and Kuo-Lun Tung. "In vitro bioactivity and antibacterial activity of strontium-, magnesium-, and zinc-multidoped hydroxyapatite porous coatings applied via atmospheric plasma spraying." *ACS Applied Bio Materials* 4, no. 3 (2021): 2523-2533. https://doi.org/10.1021/acsabm.0c01535

[38] Zuliantoni, Zuliantoni, Wahyono Suprapto, Putu Hadi Setyarini, and Femiana Gapsari. "Extraction and characterization of snail shell waste hydroxyapatite." *Results in Engineering* 14 (2022): 100390. https://doi.org/10.1016/j.rineng.2022.100390

[39] Wu, Shih-Ching, Hsi-Kai Tsou, Hsueh-Chuan Hsu, Shih-Kuang Hsu, Shu-Ping Liou, and Wen-Fu Ho. "A hydrothermal synthesis of eggshell and fruit waste extract to produce nanosized hydroxyapatite." *Ceramics International* 39, no. 7 (2013): 8183-8188. https://doi.org/10.1016/j.ceramint.2013.03.094

[40] Rodríguez-Lugo, V., T. V. K. Karthik, D. Mendoza-Anaya, E. Rubio-Rosas, L. S. Villaseñor Cerón, M. I. Reyes-Valderrama, and E. Salinas-Rodríguez. "Wet chemical synthesis of nanocrystalline hydroxyapatite flakes: effect of pH and sintering temperature on structural and morphological properties." *Royal Society Open Science* 5, no. 8 (2018): 180962. https://doi.org/10.1098/rsos.180962

[41] Varadavenkatesan, Thivaharan, Ramesh Vinayagam, Shraddha Pai, Brindhadevi Kathirvel, Arivalagan Pugazhendhi, and Raja Selvaraj. "Synthesis, biological and environmental applications of hydroxyapatite and its composites with organic and inorganic coatings." *Progress in Organic Coatings* 151 (2021): 106056. https://doi.org/10.1016/j.porgcoat.2020.106056

[42] Singh, Sanjay, Ayushi Khare, and Sanjeev Chaudhari. "Enhanced fluoride removal from drinking water using non-calcined synthetic hydroxyapatite." *Journal of Environmental Chemical Engineering* 8, no. 2 (2020): 103704. https://doi.org/10.1016/j.jece.2020.103704

[43] Boukha, Zouhair, Andoni Choya, Marina Cortés-Reyes, Beatriz de Rivas, Luis J. Alemany, Juan R. González-Velasco, José I. Gutiérrez-Ortiz, and Rubén López-Fonseca. "Influence of the calcination temperature on the activity of

hydroxyapatite-supported palladium catalyst in the methane oxidation reaction." *Applied Catalysis B: Environmental* 277 (2020): 119280. https://doi.org/10.1016/j.apcatb.2020.119280

[44] Han, Ki-Seok, Anbazhagan Sathiyaseelan, Kandasamy Saravanakumar, and Myeong-Hyeon Wang. "Wound healing efficacy of biocompatible hydroxyapatite from bovine bone waste for bone tissue engineering application." *Journal of Environmental Chemical Engineering* 10, no. 1 (2022): 106888. https://doi.org/10.1016/j.jece.2021.106888

[45] Wang, Qinshi, Yun Zhang, Xianli Zhang, Qi Li, Mingcong Huang, Shasha Huang, Qianlian Wu et al. "A Study of the Mechanism and Separation of Structurally Similar Phenolic Acids by Commercial Polymeric Ultrafiltration Membranes." *Membranes* 12, no. 3 (2022): 285. https://doi.org/10.3390/membranes12030285

[46] Feng, Shuhan, Jianyong Yi, Xuan Li, Xinye Wu, Yuanyuan Zhao, Youchuan Ma, and Jinfeng Bi. "Systematic review of phenolic compounds in apple fruits: Compositions, distribution, absorption, metabolism, and processing stability." *Journal of Agricultural and Food Chemistry* 69, no. 1 (2021): 7-27. https://doi.org/10.1021/acs.jafc.0c05481

[47] Bachmann, Suyanne Angie Lunelli, Tatiana Calvete, and Liliana Amaral Féris. "Caffeine removal from aqueous media by adsorption: an overview of adsorbents evolution and the kinetic, equilibrium and thermodynamic studies." *Science of the Total Environment* 767 (2021): 144229. https://doi.org/10.1016/j.scitotenv.2020.144229

[48] Song, Wei, David C. Markel, Sunxi Wang, Tong Shi, Guangzhao Mao, and Weiping Ren. "Electrospun polyvinyl alcohol-collagen-hydroxyapatite nanofibers: a biomimetic extracellular matrix for osteoblastic cells." *Nanotechnology* 23, no. 11 (2012): 115101. https://doi.org/10.1088/0957-4484/23/11/115101

[49] Lai, Kar Chiew, Billie Yan Zhang Hiew, Lai Yee Lee, Suyin Gan, Suchithra Thangalazhy-Gopakumar, Wee Siong Chiu, and Poi Sim Khiew. "Ice-templated graphene oxide/chitosan aerogel as an effective adsorbent for sequestration of metanil yellow dye." *Bioresource Technology* 274 (2019): 134-144. https://doi.org/10.1016/j.biortech.2018.11.048

[50] Rajahmundry, Ganesh Kumar, Chandrasekhar Garlapati, Ponnusamy Senthil Kumar, Ratna Surya Alwi, and Dai-Viet N. Vo. "Statistical analysis of adsorption isotherm models and its appropriate selection." *Chemosphere* 276 (2021): 130176. https://doi.org/10.1016/j.chemosphere.2021.130176

[51] Khandelwal, Ashish, Neethu Narayanan, Eldho Varghese, and Suman Gupta. "Linear and nonlinear isotherm models and error analysis for the sorption of kresoxim-methyl in agricultural soils of India." *Bulletin of Environmental Contamination and Toxicology* 104 (2020): 503-510. https://doi.org/10.1007/s00128-020-02803-2

[52] Bezzina, James P., Thomas Robshaw, Robert Dawson, and Mark D. Ogden. "Single metal isotherm study of the ion exchange removal of Cu (II), Fe (II), Pb (II) and Zn (II) from synthetic acetic acid leachate." *Chemical Engineering Journal* 394 (2020): 124862. https://doi.org/10.1016/j.cej.2020.124862

[53] Salehi, Narges, Ali Moghimi, and Hamidreza Shahbazi. "Preparation of cross-linked magnetic chitosan with methionine-glutaraldehyde for removal of heavy metals from aqueous solutions." *International Journal of Environmental Analytical Chemistry* 102, no. 10 (2022): 2305-2321. https://doi.org/10.1080/03067319.2020.1753718

[54] Vesali-Naseh, Masoud, Mohammad Reza Vesali Naseh, and Pegah Ameri. "Adsorption of Pb (II) ions from aqueous solutions using carbon nanotubes: A systematic review." *Journal of Cleaner Production* 291 (2021): 125917. https://doi.org/10.1016/j.jclepro.2021.125917

[55] Tsouko, Erminda, Maria Alexandri, Keysson Vieira Fernandes, Denise Maria Guimarães Freire, Athanasios Mallouchos, and Apostolis A. Koutinas. "Extraction of phenolic compounds from palm oil processing residues and their application as antioxidants." *Food Technology and Biotechnology* 57, no. 1 (2019): 29. https://doi.org/10.17113/ftb.57.01.19.5784

Name of Author	Email
Zaharah Abdul Rahman	zaharah.ar@gmail.com
Nora'aini Ali	noraaini@umt.edu.my
Sofiah Hamzah	sofiah@umt.edu.my
Syed Mohd Saufi Tuan Chik	smsaufi@ump.edu.my
Norhafiza Ilyana Yatim	hafiza.ilyana@umt.edu.my
Siti Solihah Rasdei	solihahrasdee@gmail.com
Jan Setiawan	jan.setiawan@brin.go.id